

Inclusion compounds of hydroxynaphthoic acids: co-crystal vs. salt formation†

Ayesha Jacobs,* Luigi R. Nassimbeni, Gaëlle Ramon and Baganetsi K. Sebogisi

Received 19th March 2010, Accepted 12th May 2010

DOI: 10.1039/c004458j

6-Hydroxy-2-naphthoic acid, H1, forms solvates with 1,4-dioxane (DIOX) and dimethyl sulfoxide (DMSO), and their structures are stabilized by host–host and host–guest hydrogen bonds. H1 forms a hydrated salt with 1,4-diazabicyclo[2.2.2]octane, DABCO, with stoichiometry $2\text{H1} \cdot 2\text{DABCO} \cdot 3\text{H}_2\text{O}$. Two other naphthoic acid isomers, 1-hydroxy-2-naphthoic acid, H2, and 3-hydroxy-2-naphthoic acid, H3, form salts with DABCO with host : guest ratios of 2 : 1. The kinetics of thermal decomposition of the $\text{H1} \cdot \frac{1}{2}\text{DIOX}$ compound yields an activation energy of $\sim 60 \text{ kJ mol}^{-1}$ for the desolvation reaction.

Introduction

The synthesis of multi-component molecular solids with predictable connectivities and metrics is an important current field in crystal engineering. The molecular recognition which occurs *via* hydrogen bonding depends on the relative strengths of the donor and acceptor moieties of the molecular components which are employed to synthesize the targeted co-crystals or salts. The resultant products have various applications in diverse areas of functional solids, particularly sensors, molecular filters and pharmaceuticals.^{1,2} Designing the appropriate crystallization experiments is helped by employing a number of quantitative scales which have been developed to describe the strengths of molecular interactions, such as Hunter's "Molecular Recognition Toolbox",³ Berthelot's scale of H-bond acceptor strengths,⁴ Gilli's pK slide rule,⁵ and the rules suggested by Etter.⁶ The latter have been employed with considerable success by Aakeröy^{7–9} who has successfully analyzed a number of carboxylic acid...N-heterocyclic co-crystals and salts.

Hydroxynaphthoic acids are interesting host compounds in that they have two moieties which are potential hydrogen bonding donors: carboxyl (strong) and hydroxyl (weak). We have employed three isomers of hydroxynaphthoic acid namely 6-hydroxy-2-naphthoic acid (H1), 1-hydroxy-2-naphthoic acid (H2) and 3-hydroxy-2-naphthoic acid (H3).

We exposed these host compounds to a number of solvents with different H-bond acceptor affinities. The following failed to form inclusion compounds: nitromethane, acetone, ethanol, morpholine, acetonitrile, dimethylformamide and benzylamine. Dimethyl sulfoxide (strong) and 1,4-dioxane (weak) formed complexes with H1 while pyridine was enclathrated by all three hosts. The crystals obtained, however, exhibited highly disordered structures which could not be refined satisfactorily. We therefore replaced the pyridine guest with 1,4-diazabicyclo[2.2.2]octane (strong), a bulkier molecule, which yielded satisfactory structures. The host and guest molecules are shown in Scheme 1.

Department of Chemistry, Faculty of Applied Sciences, Cape Peninsula University of Technology, PO Box 652, Cape Town, 8000, South Africa. E-mail: jacobsa@cp.uct.ac.za; Fax: +27 21 460 3854; Tel: +27 21 460 3167
† CCDC reference numbers 770706–770710. For crystallographic data in CIF or other electronic format see DOI: 10.1039/c004458j

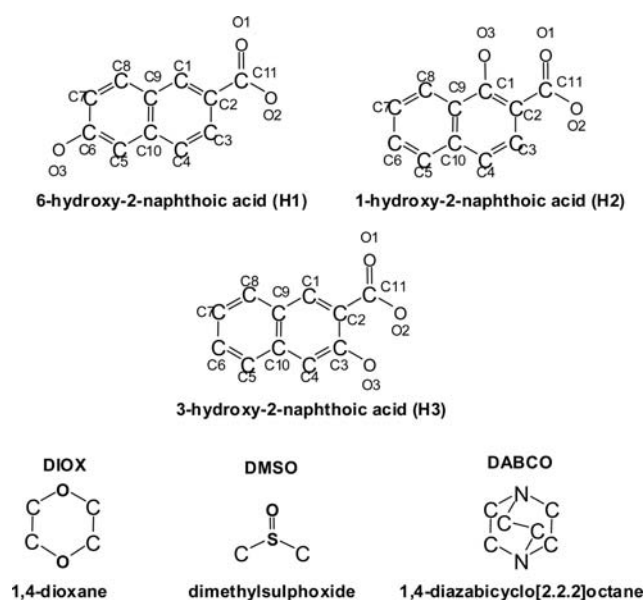
Experimental section

Crystal growth

Suitable crystals of $\text{H1} \cdot \frac{1}{2}\text{DIOX}$ and $2\text{H1} \cdot \text{DMSO}$ were obtained by slow evaporation of saturated solutions of the host and the appropriate liquid guest. Crystals of the DABCO inclusion compounds were obtained by mixing dilute solutions of the selected host and the DABCO guest using ethanol as a co-solvent. Solutions of 1 : 1 ratio of H1 : DABCO and 2 : 1 molar ratios of H2 : DABCO and H3 : DABCO were prepared. Crystals were formed after several weeks.

Structure analysis

Table 1 provides a summary of the crystal data results. The intensity data measured on a Kappa CCD diffractometer using graphite-monochromated Mo-K α radiation were used to determine the cell dimensions. The strategy for the data collections



Scheme 1 Atomic labelling scheme for hosts and schematic diagram of guests.

Table 1 Crystal data

Compound	H1 · 1/2 DIOX	2H1 · DMSO	2H1 · 2DABCO · 3H ₂ O	2H2 · DABCO	2H3 · DABCO
Structural formula	H1 ^a · 1/2 C ₄ H ₈ O	2H1 ^a · C ₂ H ₆ SO	2H1 ^a · 2C ₆ H ₁₂ N ₂ · 3H ₂ O	2H2 ^a · C ₆ H ₁₂ N ₂	2H3 ^a · C ₆ H ₁₂ N ₂
Molecular mass/g mol ⁻¹	232.23	454.48	654.75	488.52	488.52
Data collection temp./K	173(2)	173(2)	173(2)	173(2)	173(2)
Crystal system	Monoclinic	Triclinic	Monoclinic	Monoclinic	Triclinic
Space group	<i>P</i> 2 ₁ / <i>n</i>	<i>P</i> 1	<i>P</i> 2 ₁ / <i>c</i>	<i>P</i> 2 ₁ / <i>c</i>	<i>P</i> 1
<i>a</i> /Å	7.4451(4)	9.4013(10)	9.1880(18)	10.768(2)	8.6982(17)
<i>b</i> /Å	5.9568(3)	10.0069(11)	10.003(2)	24.064(5)	11.373(2)
<i>c</i> /Å	24.7267(13)	12.2414(13)	35.207(7)	9.5656(19)	11.820(2)
<i>α</i> /°	90.00	95.150(2)	90.00	90.00	85.52(3)
<i>β</i> /°	96.3190(10)	109.037(2)	91.23(3)	100.12(3)	81.69(3)
<i>γ</i> /°	90.00	90.332(2)	90.00	90.00	87.04(3)
Volume/Å ³	1089.94(10)	1085.5(2)	3234.9(11)	2440.1(9)	1152.5(4)
<i>Z</i>	4	2	4	4	2
<i>D</i> _c , Calculated density/g cm ⁻³	1.415	1.393	1.344	1.330	1.408
Absorption coefficient/mm ⁻¹	0.105	0.194	0.098	0.094	0.100
<i>F</i> (000)	488	476	1400	1032	516
<i>θ</i> range	2.79–28.31	2.29–27.60	2.12–28.38	1.92–28.46	1.75–27.56
Limiting indices	±9; ±7; ±32	±12; ±12; ±15	±12; -13; 12; -46, 47	-13, 14; ±32; ±12	±11; ±14; ±15
Reflections collected/unique	9402/2692	12 271/4861	27 354/8082	25 972/6001	8875/5102
Goodness-of-fit on <i>F</i> ²	1.082	1.041	1.044	1.029	1.031
Final <i>R</i> indices [<i>I</i> > 2σ(<i>I</i>)]	<i>R</i> ₁ = 0.0565; <i>wR</i> ₂ = 0.1782	<i>R</i> ₁ = 0.0685; <i>wR</i> ₂ = 0.1843	<i>R</i> ₁ = 0.0551; <i>wR</i> ₂ = 0.1526	<i>R</i> ₁ = 0.0418; <i>wR</i> ₂ = 0.1094	<i>R</i> ₁ = 0.0739; <i>wR</i> ₂ = 0.1195
<i>R</i> indices (all data)	<i>R</i> ₁ = 0.0656; <i>wR</i> ₂ = 0.1900	<i>R</i> ₁ = 0.0932; <i>wR</i> ₂ = 0.2046	<i>R</i> ₁ = 0.0757; <i>wR</i> ₂ = 0.1671	<i>R</i> ₁ = 0.0531; <i>wR</i> ₂ = 0.1180	<i>R</i> ₁ = 0.1777; <i>wR</i> ₂ = 0.1587
Largest diff. peak and hole/e Å ⁻³	0.628; -0.337	0.786; -0.912	0.930; -0.333	0.309; -0.196	0.245; -0.302
^a C ₁₁ H ₈ O ₃ .					

was evaluated using COLLECT software.¹⁰ For all structures, the intensity data were collected by the standard ϕ scan and omega scan techniques, scaled and reduced using the program DENZO-SMN.¹¹ The structures were solved using direct methods and refined by full-matrix least squares with SHELX-97,¹² refining on F^2 . The program X-Seed¹³ was used as a graphical interface. For all the structures the non-hydrogen atoms were found in the difference electron density map. The aromatic hydrogens of the hosts and the hydrogens of the guests not involved in hydrogen bonding were placed with geometric constraints and allowed to refine isotropically. In cases where the guest was disordered the guest hydrogen atoms were omitted. The final refinement of the hydroxylic and carboxylic hydrogens is described later in the text.

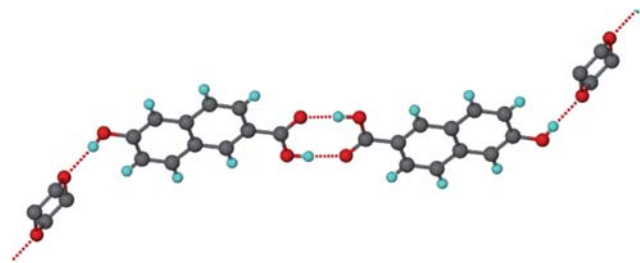


Fig. 1 Connectivity of the $\text{H1} \cdot \frac{1}{2}\text{DIOX}$ structure. The disordered carbon atoms of the dioxane are omitted for clarity.

Thermal analysis and kinetics

Both thermogravimetric analysis (TG) and differential scanning calorimetry (DSC) were performed on a Perkin Elmer 6 series system using a purge gas of nitrogen at 20 ml min^{-1} . Typical temperature ranges used were $303\text{--}633 \text{ K}$ at a heating rate of 10 K min^{-1} . For both TG and DSC the crystals were removed from the mother liquor, dried on filter paper and analysed. The sample masses were between 3 and 4 mg.

For the $\text{H1} \cdot \frac{1}{2}\text{DIOX}$ inclusion compound, the kinetics of desolvation was determined using non-isothermal methods.^{14,15} Crystals were crushed prior to analysis and a series of TG experiments with heating rates between 2 and 32 K min^{-1} were performed.

Results and discussion

The structure of $\text{H1} \cdot \frac{1}{2}\text{DIOX}$ crystallized in the space group $P2_1/n$ with $Z = 4$. The host is located in a general position while the dioxane is located on a centre of inversion. The connectivity diagram is shown in Fig. 1 in which we note the retention of the carboxylic dimer synthon connecting two H1 molecules and the (Host)OH \cdots (DIOX) hydrogen bond. Thus the weak hydroxyl donor hydrogen bonds to the weak ether oxygen acceptor. The packing is characterized by ribbons of naphthoic acid dimers centrosymmetrically connected to the dioxane and running in the [001] direction. This is the same connectivity motif found in the structure of 4-aminosalicylic acid with dioxane.¹⁶ The dioxane

Table 2 Hydrogen bonding details

Structures	Donor(D)–H \cdots acceptor(A)	D \cdots A/ \AA	D–H/ \AA	H \cdots A/ \AA	D–H \cdots A/ $^\circ$	
$\text{H1} \cdot \frac{1}{2}\text{DIOX}$	O1–H11 \cdots O2 ^a	2.651(2)	0.86(3)	1.80(1)	174(3)	
	O3–H12 \cdots O1G	2.720(2)	0.77(3)	1.98(1)	164(3)	
$\text{H1} \cdot 2\text{DMSO}$	O3A–H12A \cdots O3	2.730(3)	0.89(1)	1.84(1)	174(1)	
	O3–H12 \cdots O2G ^f	2.584(3)	0.85(1)	1.75(1)	168(4)	
$2\text{H1} \cdot 2\text{DABCO} \cdot 3\text{H}_2\text{O}$	O3–H12 \cdots S5G ^f	3.380(1)	0.85(1)	2.68(3)	141(3)	
	O4–H16 \cdots O7	2.638(2)	0.88(3)	1.78(3)	167(3)	
	O1–H1 \cdots O6 ^a	2.608(2)	0.83(3)	1.78(3)	175(3)	
	O1–H1 \cdots O5 ^a	3.158(2)	0.83(3)	2.62(3)	124(2)	
	O2–H4 \cdots O5	2.741(2)	0.77(3)	2.00(3)	163(3)	
	O2–H12 \cdots N10	2.817(2)	0.90(3)	1.94(3)	165(2)	
	O3–H7 \cdots O2	2.802(2)	0.83(3)	1.97(3)	179(3)	
	O3–H2 \cdots O6 ^b	2.787(2)	0.89(3)	1.91(4)	169(3)	
	O7–H3 \cdots O3 ^c	2.731(2)	0.90(3)	1.83(4)	176(3)	
	O7–H5 \cdots O36 ^d	2.668(3)	0.83(3)	1.88(3)	160(3)	
	N5–H6 \cdots N20	2.736(2)	0.93(1)	1.81(1)	179(2)	
	N14–H8 \cdots O11	2.559(2)	0.94(1)	1.63(1)	176(3)	
	N14–H8 \cdots O36	3.232(2)	0.94(1)	2.60(2)	125(2)	
	$2\text{H2} \cdot \text{DABCO}$	N2G–H1 \cdots O2	2.604(2)	0.95(1)	1.65(1)	177(2)
		N2G–H1 \cdots O1	3.127(2)	0.95(1)	2.52(2)	121(1)
N1G–H10 \cdots O2A		2.551(2)	0.85(1)	1.70(1)	179(4)	
N1G–H10 \cdots O1A		3.194(2)	0.85(1)	2.64(3)	124(3)	
O3–H11 \cdots O1		2.482(2)	0.95(2)	1.58(2)	155(2);	
$2\text{H3} \cdot \text{DABCO}$	O2A–H10A \cdots N1G	2.551(2)	1.01(1)	1.55(1)	171(3)	
	O3A–H11A \cdots O1A	2.536(2)	0.93(2)	1.67(2)	153(2)	
	N1G–H11A \cdots O2A	2.676(4)	1.06(1)	1.61(1)	177(3)	
	N1G–H11A \cdots O1A	3.047(3)	1.06(1)	2.39(3)	118(2)	
	O3A–H12A \cdots O2A	2.534(3)	1.09(5)	1.51(5)	153(4)	
	O3–H12 \cdots O2	2.619(3)	0.91(4)	1.81(4)	147(4)	
	O3–H12 \cdots O2 ^e	3.116(3)	0.91(4)	2.55(4)	121(3)	
	O1–H11 \cdots N2G	2.590(3)	1.16(1)	1.43(1)	177(3)	
	N2G–H11 \cdots O2	3.240(1)	1.43(1)	2.38(3)	114(2)	

^a $1 - x, 1 - y, -z$. ^b $1 - x, y, z$. ^c $1 - x, 1 - y, -z - 1$. ^d $1 - x, y - \frac{1}{2}, -z - \frac{1}{2}$. ^e $2 - x, 1 - y, 1 - z$. ^f $-x - 1, -y - 1, -z + 1$.

guests are located in channels running in the [010] direction. The metrics of the hydrogen bonding are given for this and subsequent structures in Table 2.

The stoichiometry of the dimethyl sulfoxide compound is similar to that of $\text{H1} \cdot \frac{1}{2}\text{DIOX}$. The connectivity diagram for $2\text{H1} \cdot \text{DMSO}$ is shown in Fig. 2, which displays the retention of the carboxylic acid dimers while the hydroxyl groups hydrogen bond to each other and to the DMSO guest. The latter is disordered with the sulfur in two distinct pyramidal positions with site occupancies of 0.85 and 0.15 respectively. The carboxylic hydrogens were not located and were omitted from the final model. The shortest $\text{O} \cdots \text{O}$ distances between adjacent carboxylic acid groups were 2.58(3) Å and 2.61(3) Å. We again have ribbons of the naphthoic acids which are hydrogen bonded *via* their carboxylic acid moieties and the hydroxyl moieties, running in the [011] direction.

The structure of H1 with DABCO is unusual. It crystallizes in the space group $P2_1/c$ with eight naphthoic acid anions, eight DABCO cations and twelve water molecules in the unit cell. The asymmetric unit is shown in Fig. 3. The intermolecular hydrogen bonds link a DABCO cation and a water molecule to the carboxyl anion. A second DABCO cation is hydrogen bonded to the first DABCO *via* $\text{N}-\text{H}^+ \cdots \text{N}$ hydrogen bonds. This second DABCO cation is hydrogen bonded to a second water molecule which is in turn bonded to a second naphthoic acid anion and a third water molecule. The hydroxyls of the independent naphthoic acids are in turn hydrogen bonded to repeated naphthoic acids directly or *via* water bridges.

The question of whether an acid : base pair gives rise to a co-crystal or a salt has been much discussed. The general rule is that if the $\Delta\text{p}K_{\text{a}}$ values are greater than 2 the resultant crystals will be a salt. However, $\text{p}K_{\text{a}}$ values are a measure of the proton dissociation equilibrium in aqueous solution and are not necessarily an indicative parameter in the solid state. In fact Park *et al.* have

pointed out that there is a salt : co-crystal continuum when acid–base complexes have similar $\text{p}K_{\text{a}}$ values.¹⁷ An example is pyridine and formic acid which can form either a co-crystal or a salt¹⁸ and pyridine with 3,5-dinitrobenzoic acid which forms a co-crystal as a 1 : 2 complex or a salt as a 1 : 1 : 1 complex with additional water.¹⁹ In our case $\Delta\text{p}K_{\text{a}}$ is 3.9 for H1 : DABCO and 5.2 for H2/H3 : DABCO. We therefore expect to form salts.

Additional information can be gained by measuring the differences in the C–O distances in the carboxylic moieties. In general if these are between 0.08 and 0.12 Å this indicates a co-crystal while smaller differences of less than 0.04 Å are more typical of the salt.

Noting these difficulties we took particular care in the refinement of the structures $2\text{H2} \cdot \text{DABCO}$ and $2\text{H3} \cdot \text{DABCO}$. The difference between a co-crystal and a salt is subtle, and dependent upon the location of the hydrogen atom. We therefore adopted the following strategy in the refinement of these structures: all heavy atoms were refined anisotropically. Hydrogen atoms attached to the carbons were placed geometrically and the hydroxyl hydrogens which are involved in intramolecular hydrogen bonding were refined independently. The hydrogens involved in intermolecular hydrogen bonding were initially omitted from the model and their location established by electron difference maps. They were subsequently refined with bond length constraints to their parent atoms.

The $2\text{H2} \cdot \text{DABCO}$ structure (Fig. 4) crystallizes in $P2_1/c$ with $Z = 4$. There are thus two hosts and one DABCO in the asymmetric unit. The result is ambiguous, the naphthoic acid host labelled A has $\Delta D_{\text{CO}} = 0.004$ Å and we located a proton on the DABCO base with an N–H distance of 0.95(1) Å. For naphthoic acid B the $\Delta D_{\text{CO}} = 0.040$ Å and we located two possible peaks for the hydrogen, one with an N–H distance of 0.85(1) Å and the other at 1.01(1) Å from the carboxylic oxygen. This implies the possibility of DABCO being doubly protonated, a result that has

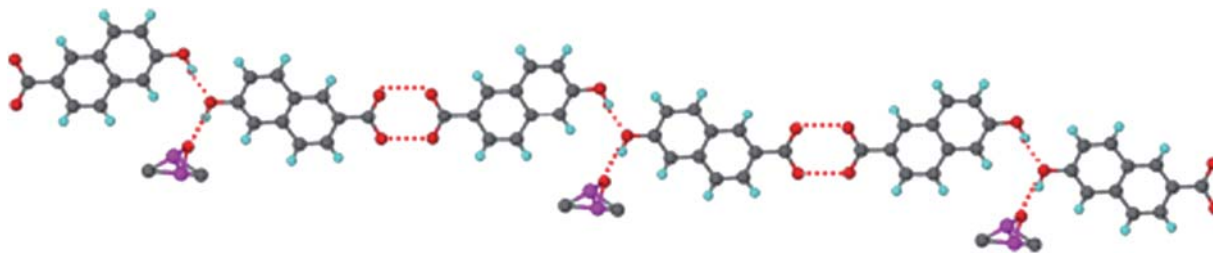


Fig. 2 Connectivity diagram of $2\text{H1} \cdot \text{DMSO}$.

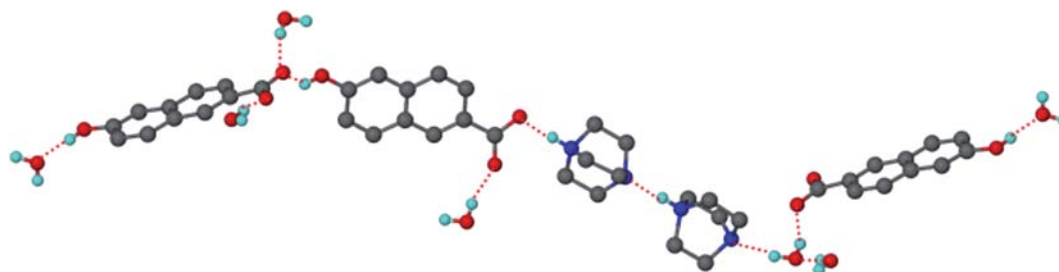


Fig. 3 Hydrogen bonding scheme in $2\text{H1} \cdot 2\text{DABCO} \cdot 3\text{H}_2\text{O}$. Only H-bonded hydrogens are shown.

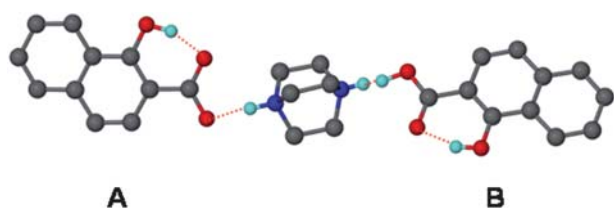


Fig. 4 Hydrogen bonding scheme in $2H_2 \cdot DABCO$. Only H-bonded hydrogens are shown.

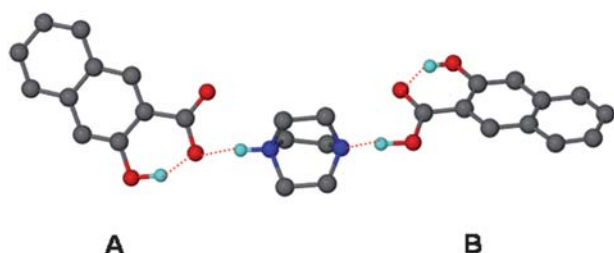


Fig. 5 Asymmetric unit of $2H_3 \cdot DABCO$. Only H-bonded hydrogens are shown.

been previously established, as shown by the salts formed with malonic acid,²⁰ fumaric²¹ and oxalic acid.²²

The results obtained for $2H_3 \cdot DABCO$ are found in Fig. 5. The structure of $2H_3 \cdot DABCO$ crystallizes in $P\bar{1}$ with $Z = 2$. Naphthoic acid A again forms a salt with DABCO with an N–H distance of 1.06(1) Å, with the ΔD_{co} uncharacteristically large at 0.079 Å. The naphthoic acid B is not ionized, ΔD_{co} is 0.080 Å and the O–H distance is 1.16(1) Å.

Thermal analysis and kinetics

The thermal analysis results are shown in Table 3. There is good agreement between the calculated and the experimental mass losses for the dioxane compound (less than 1%). The experimental value for the dimethyl sulfoxide compound is considerably larger than the calculated value due to the presence of surface DMSO. Both of the DSC curves show two endotherms, the first due to the loss of guest followed by the host melt.

The $2H_1 \cdot 2DABCO \cdot 3H_2O$ compound has a complex thermogravimetry curve which shows a mass loss of 16% up to 473 K with a corresponding endotherm in the DSC. We surmise that this is due to both the loss of water and a partial loss of DABCO since the latter sublimates from 323 K.

Table 3 Thermal analysis data

Inclusion compound	$H_1 \cdot \frac{1}{2}DIOX$	$2H_2 \cdot DMSO$	$2H_1 \cdot 2DABCO \cdot 3H_2O$	$2H_2 \cdot DABCO$	$2H_3 \cdot DABCO$
H : G ratio	1 : $\frac{1}{2}$	1 : $\frac{1}{2}$	2 : 2 : 3	1 : $\frac{1}{2}$	1 : $\frac{1}{2}$
TG (calc % mass loss)	20.0	17.1	—	—	—
TG (exp % mass loss)	19.5	19.6	—	—	—
DSC (T_{on})/K					
A	400.9	377.7	387.2	428.1	483.8
B	519.2	516.6	466.6	501.5	562.0
C	—	—	564.3	—	—

Both the $2H_2 \cdot DABCO$ and the $2H_3 \cdot DABCO$ DSC curves exhibit endotherms which do not correspond to that of the host or the guest melts confirming that a new compound was formed.

The kinetics of desolvation of the dioxane compound was determined using non-isothermal methods. The resultant TG curves (Fig. 6) were analysed and a further plot of $\log \beta$ vs. $1/T$ (Fig. 7), where β is the heating rate, gave a range of activation energies, 58–63 kJ mol⁻¹. It is difficult to compare activation energies of desolvation reactions in inclusion compounds, as they are dependent on a number of factors such as the topology of the space in which the guest is included, the nature of the guest, its molar mass, boiling point and the number and strengths of the host–host and host–guest interactions which occur in the crystal structure.

We note that in the structures formed between 2,2'-dihydroxy-1,1'-binaphthyl and 1,4-dioxane,²³ the compound with a guest : host (G : H) ratio of 3.5 has the 1,4-dioxane located in channels and yields an activation energy of desolvation of 61 kJ mol⁻¹ while the inclusion compound with G : H ratio of 1.5 had an activation energy of 86 kJ mol⁻¹. The host 9,9'-(biphenyl-4,4'-diyl)-bis(flouren-9-ol) forms an inclusion compound with dioxane with G : H ratio of 3 which decays in a single step with $E_a = 95.5$ kJ mol⁻¹ and the dioxane molecules are in restricted channels.²⁴ The structure of the inclusion compound of dioxane with 9-(1-naphthyl)-9H-xanthen-9-ol,²⁵ with a stoichiometry of 1 : 1 is a true clathrate, with the dioxane guest located in cages created by

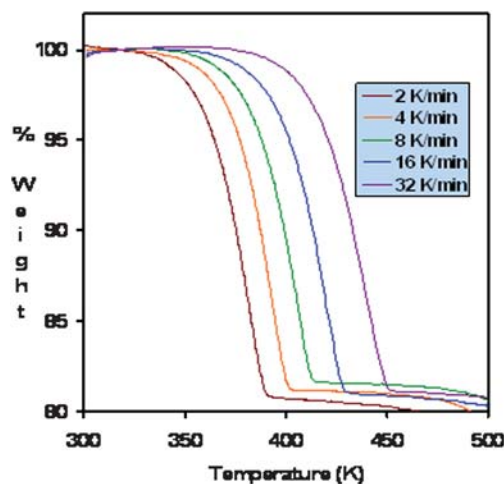


Fig. 6 Non-isothermal results for the desolvation of $H_1 \cdot \frac{1}{2}DIOX$.

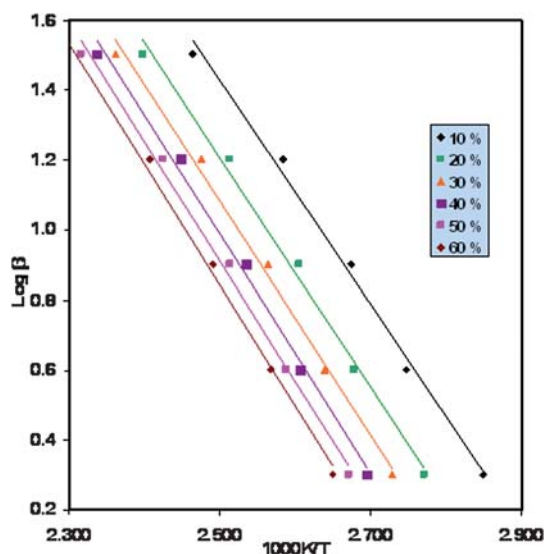


Fig. 7 Plot of $\log \beta$ vs. $1/T$ for $\text{H1} \cdot \frac{1}{2}\text{DIOX}$. The decomposition stages from 10–60% were analysed.

the host framework. Its decomposition yielded an activation energy E_a of 111 kJ mol^{-1} .

Conclusion

Hydroxynaphthoic acids are interesting host compounds in that they possess hydrogen bonding moieties of differing donor strengths. In the case of the solvate structures obtained with dioxane and dimethyl sulfoxide, the carboxylic acid dimer synthon is retained and the guests are stabilized by $\text{OH} \cdots \text{O}(\text{Guest})$ hydrogen bonds using the phenolic hydroxy group. The structures with DABCO are salts in which the carboxylate anions are hydrogen bonded to the protonated DABCO via $(\text{Host})\text{-COO}^- \cdots \text{H-N}^+(\text{Guest})$ hydrogen bonds. However, in the case of $2\text{H2} \cdot \text{DABCO}$, there is an ambiguity arising from two peaks corresponding to a disordered hydrogen located in the vicinity of a DABCO nitrogen and a carboxylic oxygen. The activation energy of the desolvation reaction of $\text{H1} \cdot \frac{1}{2}\text{DIOX}$ is in the expected range of inclusion compounds of this kind, in which the guests are located in channels.

Acknowledgements

We thank the NRF (Pretoria) and the Cape Peninsula University of Technology for funding.

Notes and references

- Ó. Almarsson and M. J. Zaworotko, *Chem. Commun.*, 2004, 1889.
- C. B. Aakeröy, N. C. Schultheiss, A. Rajbanshi, J. Desper and C. Moore, *Cryst. Growth Des.*, 2009, **9**, 432.
- C. A. Hunter, *Angew. Chem., Int. Ed.*, 2004, **43**, 5310.
- C. Lawrence and M. Berthelot, *Perspect. Drug Discovery Des.*, 2000, **18**, 39.
- P. Gilli, L. Pretto, V. Bertolasi and G. Gilli, *Acc. Chem. Res.*, 2009, **42**, 33.
- M. C. Etter, *Acc. Chem. Res.*, 1990, **23**, 120.
- C. B. Aakeröy, J. Desper and J. F. Urbina, *Chem. Commun.*, 2005, 2820.
- C. B. Aakeröy, J. Desper and M. E. Fasulo, *CrystEngComm*, 2006, **8**, 586.
- C. B. Aakeröy, I. Hussain, S. Forbes and J. Desper, *CrystEngComm*, 2007, **9**, 46.
- COLLECT, *Data Collection Software*, Nonius, Delft, The Netherlands, 1998.
- Z. Otwinowski and W. Minor in *Methods in Enzymology, Macromolecular Crystallography*, ed. C. W. Carter, Jr and R. M. Sweet, Academic Press, 1997, part A, vol. 276, pp. 307–326.
- G. M. Sheldrick, *SHELX-97: Program for Crystal Structure Refinement*, University of Göttingen, Germany, 1997.
- L. J. Barbour, X-Seed: a Software Tool for Supramolecular Crystallography, *J. Supramol. Chem.*, 2001, **1**, 189.
- J. H. Flynn and L. A. Wall, *J. Polym. Sci., Part B: Polym. Lett.*, 1966, **4**, 323.
- T. Ozawa, *Bull. Chem. Soc. Jpn.*, 1965, **38**, 1881.
- V. André, D. Braga, F. Grepioni and M. T. Duarte, *Cryst. Growth Des.*, 2009, **9**, 5108.
- S. L. Childs, G. P. Stahly and A. Park, *Mol. Pharmaceutics*, 2007, **4**, 323.
- D. Wiechert and D. Mootz, *Angew. Chem., Int. Ed.*, 1999, **38**, 1974.
- K. K. Arora, J. PrakashaReddy and V. R. Pedireddi, *Tetrahedron*, 2005, **61**, 10793.
- D. Braga and L. Maini, *Chem. Commun.*, 2004, 976.
- R. Gobetto, C. Nervi, M. R. Chierotti, D. Braga, L. Maini, F. Grepioni, R. K. Harris and P. Hodgkinson, *Chem.-Eur. J.*, 2005, **11**, 7461.
- R. Vaidyanathan, S. Natarajan and C. N. R. Rao, *J. Mol. Struct.*, 2002, **608**, 123.
- L. R. Nassimbeni and H. Su, *J. Phys. Org. Chem.*, 2000, **13**, 368.
- M. R. Caira, T. le Roex, L. R. Nassimbeni, J. A. Ripmeester and E. Weber, *Org. Biomol. Chem.*, 2004, **2**, 2299.
- A. Jacobs, L. R. Nassimbeni and B. Taljaard, *Acta Crystallogr., Sect. C: Cryst. Struct. Commun.*, 2004, **60**, o668.